

## Initial growth of Bi films on a Si(111) substrate: Two phases of $\sqrt{3} \times \sqrt{3}$ low-energy-electron-diffraction pattern and their geometric structures

K. J. Wan, T. Guo,\* W. K. Ford,<sup>†</sup> and J. C. Hermanson

*Advanced Materials Center and Department of Physics, Montana State University, Bozeman, Montana 59717*

(Received 19 April 1991)

The ordering of Bi on a Si(111)- $7 \times 7$  surface was studied as a function of overlayer coverage and deposition conditions using low-energy electron diffraction (LEED) and Auger electron spectroscopy. We observed a one-third-monolayer and a saturated one-monolayer phase. Both phases displayed identical  $\sqrt{3} \times \sqrt{3}$ - $R30^\circ$  LEED symmetries. LEED intensity data were used to differentiate between the two phases and to determine a quantitative atomic geometry via a thorough dynamical LEED analysis.

The structural characterization of column-III and -V elements deposited on semiconductor substrates continues to be a major subject of study. This interest is driven in part by the desire to improve III-V epitaxy on silicon for application to the manufacture of microelectronics.<sup>1</sup> The Si(111) surface is one of the most thoroughly studied substrates. It is known that atomic reconstruction occurs for the free surface of Si(111) and that this reconstruction can be significantly modified by the presence of adatom impurities even at trace, submonolayer concentration. The physical origin of surface reconstruction can be understood as a minimization of the surface free energy. The Si(111)- $1 \times 1$  surface with all atoms located at their ideal bulk positions is not realized since it would have too many energetically costly dangling bonds. The  $2 \times 1$  and  $7 \times 7$  reconstructions are stabilized electronically by the removal of surface dangling bonds, leading to a subtle change in the surface atomic geometry.<sup>2</sup> The introduction of covalently bonded adatoms introduces an additional term in the surface free energy, that passivates the surface dangling bonds. Column-III (Al, Ga, In) adatoms generally induce a  $\sqrt{3} \times \sqrt{3}$ - $R30^\circ$  (called  $\sqrt{3} \times \sqrt{3}$  hereafter) reconstruction on the Si(111) surface by bonding at the  $T_4$  site directly above second-layer Si atoms.<sup>3-5</sup> The column-V metal As, on the other hand, stabilizes a  $1 \times 1$  surface cell by substituting for the topmost (absent) Si atom.<sup>6</sup> One might expect As-like reconstructions to occur upon adsorbing other column-V elements such as Sb and Bi. Instead, both Sb and Bi adatoms induce a  $\sqrt{3} \times \sqrt{3}$  structure; no well-ordered  $1 \times 1$  structure has been reported. Recent x-ray-diffraction and scanning-tunnel microscope (STM) studies show that the  $\sqrt{3} \times \sqrt{3}$  reconstruction involves adatom trimers at each  $\sqrt{3} \times \sqrt{3}$  site, at one monolayer (ML) coverage.<sup>7,8</sup> This trimer model disagrees with the model of  $\frac{1}{3}$ -ML saturated coverage proposed earlier by Kawazu *et al.*<sup>9</sup> However, x-ray-diffraction results are ambiguous with respect to a  $180^\circ$  rotation of the Si(111) surface.<sup>10</sup> Therefore, the atomic configuration responsible for the  $\sqrt{3} \times \sqrt{3}$  reconstruction on an atomic scale has not been determined. In this paper, we present results from low-energy electron diffraction (LEED) and Auger electron spectroscopy (AES) studies which show that two distinct phases form the  $\sqrt{3} \times \sqrt{3}$  superlattice in the Bi/Si(111) system. The Bi

coverage necessary for the completion of each phase was determined to be about  $\frac{1}{3}$  and 1 ML and the substrate temperatures corresponding to each phase are  $\sim 360^\circ\text{C}$  and  $\sim 300^\circ\text{C}$ , respectively. On the basis of quantitative comparison between experimental and theoretical  $I$ - $V$  spectra calculated by multiple-scattering theory, we report that (1) at  $\frac{1}{3}$  ML, Bi atoms adsorb on the  $T_4$  site, and (2) at 1 ML, Bi atoms form trimer clusters centered on the  $T_4$  position; significant deformation of the first two atomic Si layers is implied in both cases. Detailed atomic coordinates are given for the top two Si layers.

The experimental chamber was equipped with four-grid LEED optics which were also used as a retarding field analyzer for the AES measurement. The computer-controlled video LEED optics and the experimental conditions were the same as described in previous work.<sup>11</sup> The incident electron beam was aligned within  $\sim 0.5^\circ$  of the sample normal as permitted by our instrument.<sup>11</sup> The samples were cooled to  $\sim 125^\circ\text{C}$  before the  $I$ - $V$  curves were measured. Si(111) wafers were cleaned by repeated flashing at high temperatures. After cleaning, a sharp  $7 \times 7$  LEED pattern was observed, and no impurities were detected by AES.

The production of either reconstruction requires thermal annealing after metal deposition. Therefore, the temperature of the Bi-covered surface was monitored. This surface was produced by 3-ML Bi deposition on a clean Si(111)- $7 \times 7$  substrate kept at room temperature. The annealing temperature was increased from room temperature to about  $500^\circ\text{C}$ , when the Bi was believed to be desorbed. For every increment of  $20^\circ\text{C}$  and 2 min, the LEED pattern was recorded and  $I$ - $V$  spectra were measured. After metal deposition, the  $7 \times 7$  pattern is replaced by a very weak and diffuse  $1 \times 1$  pattern. Annealing reduces the background intensity and a  $\sqrt{3} \times \sqrt{3}$  pattern began to appear at  $\sim 220^\circ\text{C}$  and appeared very clearly at  $300^\circ\text{C}$ . However, upon further annealing in the range of  $300$ - $360^\circ\text{C}$ , the intensity of the spots decreased slightly and, surprisingly, became very clear again after passing  $360^\circ\text{C}$ . Comparison of two sets of  $I$ - $V$  curves, taken at  $300$  and  $360^\circ\text{C}$ , showed quite different features, which indicates different structures must be involved. In order to confirm the existence of two distinct phases, the following sample preparations were made to determine the saturat-

ed Bi coverage and corresponding substrate temperature: (i) 1-, 2-, and 3-ML bismuth were deposited, respectively, on a clean  $7\times 7$  room temperature substrate, followed by annealing to about  $300^\circ\text{C}$ . (ii)  $\frac{1}{2}$ -, 1-, and 2-ML bismuth were deposited, respectively, on a clean room-temperature substrate, followed by annealing to about  $360^\circ\text{C}$ . (iii) 3-ML Bi was deposited on a clean substrate kept at  $300^\circ\text{C}$ . (iv) 2-ML Bi was deposited on a clean substrate kept at  $360^\circ\text{C}$ .

For each sample, AES measurements were used to monitor the Bi coverage. Figure 1 shows the results of those measurements; the Auger line intensity was calibrated for a 1-ML film by using a quartz-crystal oscillator. The Auger measurements from the third and fourth samples implied Bi coverages of about 1 and  $\frac{1}{3}$  ML, respectively. The observations of LEED patterns and the measurements of  $I$ - $V$  curves for each sample prepared above confirmed our previous observations. The following conclusions can be drawn.

(i) The  $I$ - $V$  curves from the first and third samples are essentially identical, as are those from the second and fourth samples.

(ii) Each phase has a unique saturation coverage. As long as the substrate remains at a specified temperature, only  $\frac{1}{3}$  or 1-ML Bi coverage remains on the surface. This behavior is in good agreement with thermal-desorption experiments by Kawazu *et al.*,<sup>9</sup> although their observed temperature dependence is somewhat different. They observed a dip in the desorption flux of Bi when the substrate was at  $\sim 460^\circ\text{C}$  and also recorded a plateau between 250 and  $300^\circ\text{C}$ .

(iii) The two  $\sqrt{3}\times\sqrt{3}$  structures are stable and reproducible. Small changes in the coverage and the substrate temperature affect only the intensity of each beam. The major features of the  $I$ - $V$  curves are almost identical for a given phase.

(iv) The  $\beta$ -phase structure of 1-ML Bi at  $300^\circ\text{C}$  substrate temperature can be transformed to the  $\alpha$  phase of  $\frac{1}{3}$ -ML Bi at higher temperatures. In this process Bi adatoms are removed from the surface by thermal desorption.

(v) The intensity of individual LEED beams has turn-

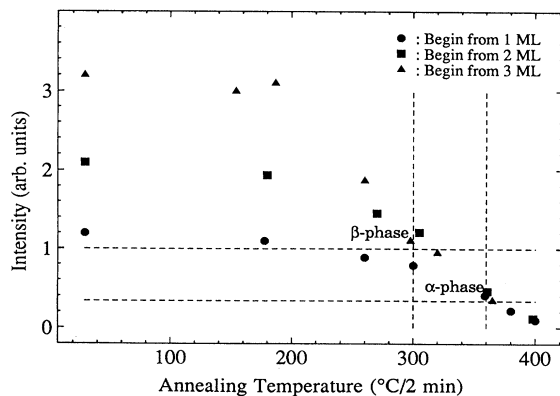


FIG. 1. Bi (96 and 101 eV) Auger line intensity vs annealing temperature for 1.5-ML coverage on Si(111) surface. The range of observed LEED symmetry is also indicated.

ing points during the thermal annealing of the first and second samples. When the temperature exceeded  $\sim 300^\circ\text{C}$  and  $\sim 360^\circ\text{C}$  the intensity of beams increased markedly.

In Figs. 2 and 3, the solid lines show the  $I$ - $V$  curves of the  $\alpha$  phase and  $\beta$  phase obtained from the fourth and third samples, respectively, for five integral-order [Figs. 2(a) and 3(a)] and four fractional-order [Figs. 2(b) and 3(b)] beams. Obviously, they exhibit quite different features. We find that the  $\sqrt{3}\times\sqrt{3}$  structure achieved by deposition on the hot substrate gives better stability and reproducibility for both phases; accordingly, we have used these data for the multiple-scattering analysis.

Dynamical calculations of  $I$ - $V$  curves for the Bi-

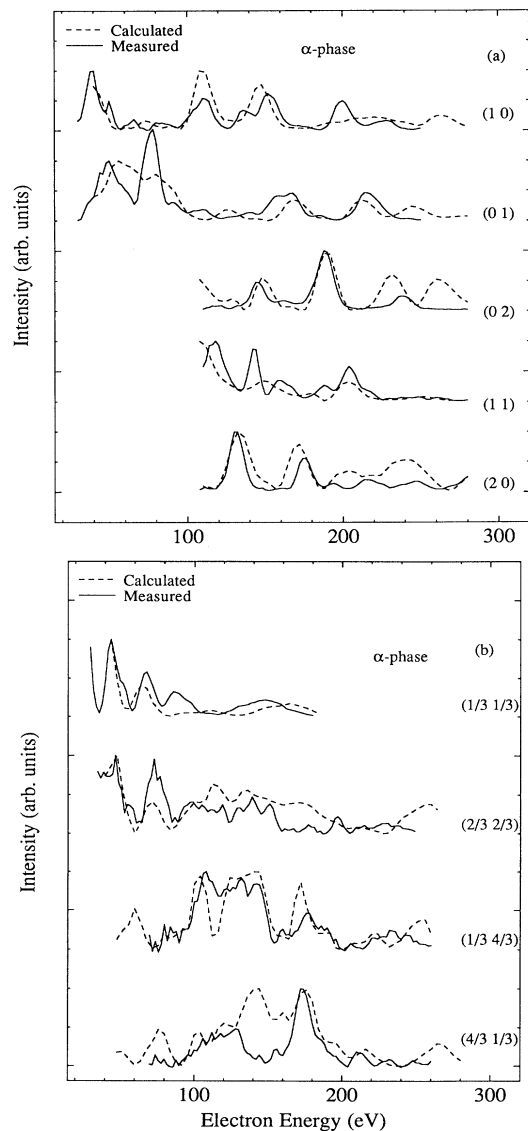


FIG. 2. Comparison between experimental and calculated  $I$ - $V$  spectra for the  $\alpha$  phase. Solid curves are taken from experimental data and dashed lines are the computed intensities of the best fit structural model in Fig. 4. (a) Integral spots. (b) Fractional spots. Averaged  $R_x$  (eleven beams) is 0.233.

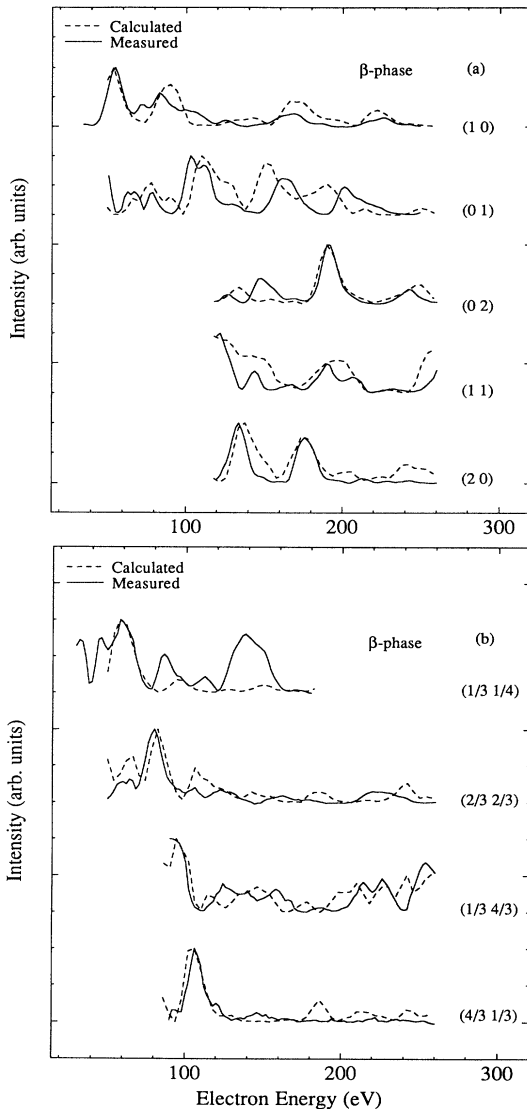


FIG. 3. Same as in Fig. 2, except for the  $\beta$  phase. Averaged  $R_x$  is 0.225.

Si(111)- $\sqrt{3}\times\sqrt{3}$  surfaces were performed to determine the atomic configurations responsible for each phase. We used a modified computer source code based on the method of Duke and Laramore and reported elsewhere.<sup>12</sup> The calculation used six phase shifts; both the imaginary and real parts of the inner potential were varied. A set of geometric parameters were selected to vary the adatom height and the substrate-atom relaxation in both perpendicular and parallel directions. The x-ray reliability factor  $R_x$  is the figure of merit used in the calculations discussed below to compare the calculated and experimental  $I$ - $V$  data sets.<sup>13</sup> For the  $\alpha$  phase with a Bi coverage of  $\frac{1}{3}$  ML, we tested the  $T_4$ ,  $H_3$ , and top-layer models proposed in the literature. The  $T_4$  model produced calculated  $I$ - $V$  curves in best agreement with the experimental data. All other models can be ruled out since they yield poor  $R_x$  ( $R_x=0.38$  for the  $H_3$  and  $R_x=0.44$  for the top-layer model). In the  $T_4$  model, the Bi atom adsorbs at the  $T_4$

site and induces the initial Si bilayer deformation. The comparison between the experimental and theoretical  $I$ - $V$  spectra for the  $T_4$  model are shown with dashed lines in Fig. 2. The value of  $R_x$  averaged over all nine beams is 0.233. For the  $\beta$  phase with 1-ML Bi coverage, the trimer model proposed by Takahashi was tested.<sup>7</sup> In this model, the center of the trimer could be located either on the  $T_4$  site or on the  $H_3$  site. The  $T_4$  site produced the best fit, the overall  $R_x$  was 0.225, while the value of 0.41 for  $R_x$  is the best that can be obtained for the  $H_3$  site. Dashed lines in Fig. 3 show the calculated  $I$ - $V$  spectra in comparison with experiment. Figures 4(a) and 4(b) show the top view and side view of the  $T_4$  and trimer models together with the directions of substrate relaxation. The atomic configuration of the optimal structures is expressed in terms of the bond lengths and vertical distances among the initial two bilayer atoms. The vertical distance of atoms 6 and 8 was assumed to be the bulk value and all other atoms beyond the fourth layer are assumed to remain at their bulk position. Table I summarizes our optimal results and corresponding bulk values.

In the optimized structures of the  $T_4$  and trimer models, the three nearest Si neighbors to the Bi atom or trimer (atoms 2,3 in Figs. 4 and another atom not shown) are slightly squeezed together, and the second-layer atom beneath the adatom (atom 5) is displaced strongly downward. This, in turn, causes the third-layer atom beneath the adatom (atom 7) to be displaced downward, and the atoms surrounding the hollow site (e.g., atom 4) to move upward. As a result, the bond length between atoms 4 and 6 is elongated, and that between atoms 5 and 7 is shortened, relative to the bulk values. Although the  $z$

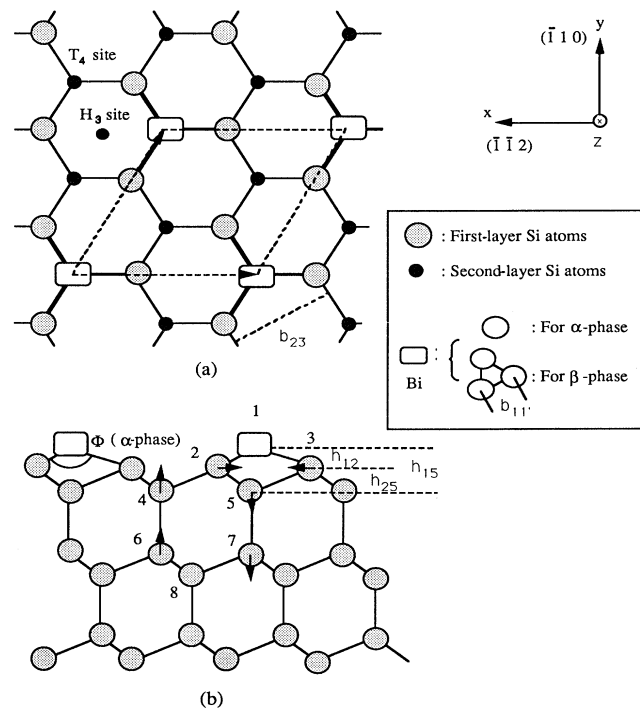


FIG. 4. (a) Top and (b) side views of the optimized structures for the  $\alpha$  and  $\beta$  phases: The  $T_4$  and trimer model.

TABLE I. Optimal structures for the  $\alpha$  and  $\beta$  phases. The parameters are defined according to Fig. 4; e.g.,  $b_{11'}$  is the side of trimer and  $b_{12}$  is the bond length between atoms 1 and 2, etc.

Parameters	$b_{11'}$ (Å)	$b_{12}$ (Å)	$b_{23}$ (Å)	$b_{25}$ (Å)	$b_{24}$ (Å)	$b_{57}$ (Å)	$b_{46}$ (Å)	$h_{12}$ (Å)	$h_{15}$ (Å)	$h_{25}$ (Å)	$\Phi$ (deg)
Bulk values	2.92 <sup>a</sup>	2.57 <sup>a</sup>	3.840	2.350	2.350	2.350	2.350		2.57 <sup>a</sup>		
$\alpha$ phase		2.388	3.667	2.504	2.350	2.239	2.476	1.107	2.445		100.3
$\beta$ phase	2.928	2.248	3.635	2.377	2.322	2.239	2.357	2.210		1.116	

<sup>a</sup>Sum of covalent radii.

coordinate of any individual atom may change significantly from its bulk value, and average height of each substrate layer remains close to its value in the bulk.

A simple explanation of the observed surface reconstructions follows from surface-energy arguments. When a foreign adatom such as Bi is deposited on a clean Si(111) surface, the density of the dangling bonds can be reduced, therefore the surface energy is reduced. Each adatom bonds to three surface atoms. For Bi, the bonding is tetrahedrally coordinated and exhibits  $p^3$  character. In the  $T_4$  model, a single Bi atom has three  $p$  bonds to the nearest neighbors of the initial Si atomic layer and two  $s$ -like orbitals form a lone pair. However, in the trimer, the  $p$ -like orbitals from the three Bi atoms must have a bond angle of  $60^\circ$  within the trimer extending downward to the substrate. These orbitals may simply saturate the three dangling bonds of the substrate to form a  $\sqrt{3} \times \sqrt{3}$  structure. Thus, either the  $T_4$  model for the  $\alpha$  phase or the trimer model for the  $\beta$  phase can easily passivate the dangling bonds. The substrate relaxations are energetically favorable since such displacements allow the Bi atom to move closer to the Si surface atoms; this optimizes the distances between the Bi and the four nearest Si atoms, these distances being near the sum of the covalent radii of Bi and Si (2.57 Å) for the  $T_4$  model.

Since the interaction between the Bi and Si atoms depends on the bonding environment, the structure of the surface is expected to be temperature dependent. In thermal-desorption experiments, Kawazu *et al.*<sup>9</sup> concluded that Bi has two-dimensional adlayer growth with a  $\sqrt{3} \times \sqrt{3}$  structure at 740 K and three-dimensional island growth below 640 K. From our experiment, we conclude that there is another phase below 640 K, distinct from the one at high temperature; both phases exhibit an identical  $\sqrt{3} \times \sqrt{3}$  LEED pattern. Our picture of the growth of Bi overlayers on Si(111) surfaces can be summarized as follows. At high coverage and a certain substrate temperature, the adsorbed Bi atoms are bonded to the hollow site above the second Si atomic layer and form a trimer clus-

ter, in agreement with x-ray analysis and STM observation.<sup>7</sup> These Bi atoms induce substrate relaxation, resulting in Si atoms moving toward the trimer center. In this way, the coexistence of Bi-Si attractive bonding and Bi-Bi, Si-Si repulsion reaches equilibrium. When the substrate temperature is increased, the extra surface energy enhances the repulsive forces and leads to the breaking of the Bi-Bi bonds because of the lower Bi-Bi single-bond energy.<sup>14</sup> A new equilibrium is achieved, in which the higher temperature removes excess Bi atoms and another reconstruction (the  $T_4$  model already described) occurs which reduces surface lateral reconstruction ( $b_{23}$  increases from 3.635 to 3.667 Å to approach the bulk value of 3.84 Å). When the substrate is kept at  $360^\circ\text{C}$ , the repulsive forces dominate and only  $\frac{1}{3}$ -ML Bi remains on the surface. At higher temperatures, impinging Bi atoms are reevaporated and no film growth can be obtained. This is in good agreement with desorption experiments.<sup>9</sup>

In summary, we have presented results showing that the actual surface geometry of the Si(111)- $\sqrt{3} \times \sqrt{3}$  Bi surface consists of two different phases, one at  $\frac{1}{3}$  ML, and another at 1 ML. The geometries for both phases are shown in Fig. 4. In the  $\alpha$  phase, the Bi atoms are adsorbed on the  $T_4$  sites at 1.106 Å above the initial Si atomic layer, which shows deformation. In the  $\beta$  phase, the structure surface consists of Bi trimers at each  $\sqrt{3} \times \sqrt{3}$  site with an interatomic distance of 2.93 Å. The center location of the trimer lies directly above the second-layer atom of the Si substrate with a spacing of 2.210 Å between the Bi layer and the ideal initial Si layer. Both numbers are slightly smaller than those obtained from x-ray-diffraction experiments.<sup>7</sup> The phenomenon of transitions from one surface reconstruction to another should provide interesting studies bearing on those factors that lead to the surface stress and the energetic properties of interface formation.

This work was supported by National Science Foundation Grant No. DMR-8705879, and by the National Center for Supercomputing Applications.

\*Present address: Research and Development, Gould AMI Semiconductors, 2300 Buckskin Road, Pocatello, ID 83210.

†Present address: Intel Corporation, 5200 NE Elam Young Pkwy, M/S AL3-15, Hillsboro, OR 97124.

<sup>1</sup>L. J. Brillson, Surf. Sci. Rep. **2**, 123 (1982).

<sup>2</sup>R. D. Meade and D. Vanderbilt, Phys. Rev. B **40**, 3905 (1989).

<sup>3</sup>J. E. Northrup, Phys. Rev. Lett. **53**, 683 (1984).

<sup>4</sup>A. Kawazu and H. Sakama, Phys. Rev. B **37**, 2704 (1988).

<sup>5</sup>J. M. Nicholls, B. Reihl, and J. E. Northrup, Phys. Rev. B **35**, 4137 (1987).

<sup>6</sup>R. I. G. Uhrberg *et al.*, Phys. Rev. B **35**, 3945 (1987).

<sup>7</sup>T. Takahashi *et al.*, Surf. Sci. **191**, L191 (1987).

<sup>8</sup>P. Mårtensson *et al.*, Phys. Rev. B **42**, 7230 (1990).

<sup>9</sup>A. Kawazu *et al.*, Surf. Sci. **86**, 108 (1979).

<sup>10</sup>J. S. Pedersen *et al.*, Surf. Sci. **189**, 1047 (1987).

<sup>11</sup>T. Guo, R. E. Atkinson, and W. K. Ford, Rev. Sci. Instrum. **61**, 968 (1990); W. K. Ford *et al.*, Phys. Rev. B **42**, 8952 (1990).

<sup>12</sup>K. J. Wan, T. Guo, and W. K. Ford (unpublished).

<sup>13</sup>E. Zanazzi and F. Jona, Surf. Sci. **62**, 61 (1977).

<sup>14</sup>See L. Pauling, *The Chemical Bond* (Cornell Univ. Press, Ithaca, 1967).